JOURNAL OF CATALYSIS 157, 235–243 (1995)

Titanium Boralites with MFI Structure Characterized Using XRD, XANES, IR, and UV–Visible Techniques: Effect of Hydrogen Peroxide on the Preparation

D. Trong On,*,† S. Kaliaguine,† and L. Bonneviot*,[1]

Department of Chemistry, Department of Chemical Engineering,† and CERPIC, Laval University, Ste Foy, G1K 7P4, Canada*

Received March 14, 1995; revised July 27, 1995; accepted July 28, 1995

Peroxytitanate, boric acid, and a controlled excess of hydrogen peroxide have been added to the preparation mixture of silicalites to synthesize titanium boralites, TBS-1, of MFI structure. After crystallization, the unit cell expansion at a constant boron substitution level of 2.7% indicates that titanium is, like boron, incorporated in the framework. The simultaneous incorporation of Ti and B is confirmed by characteristic IR bands at 920, 960, and 1380 cm^{-1}. Reflectance UV–visible spectroscopy reveals that, in the presence of boron, there is always a formation of extraframework oxide clusters with an anatase-like structure identified by XANES at the Ti K-edge. The striking similarity between the Ti K-edges of framework tetrahedral Ti sites in TBS-1 and boron-free TS-1 indicates that the sites are more likely identical in both materials. A quantification of the extraframework Ti species from the edges clearly evidences that, in the presence of boron, more hydrogen peroxide is necessary in the gel to optimize the incorporation of Ti in the framework.

1. INTRODUCTION

Since the discovery of the unique catalytic properties of titanium silicalites in selective oxidation reactions using hydrogen peroxide, there have been several attempts to incorporate another ion along with Ti^{4+} to modify their catalytic properties. Coincorporation of titanium and trivalent metal ions such as B^{3+}, Al^{3+}, Ga^{3+}, and Fe^{3+} in MFI and MEL structures has been reported recently (1–5). In some cases, a sequential approach has been adopted; boron has been partly replaced by titanium in a postsynthesis modification sequence of beta boralites (6). These modified silicalites are active both in oxidation reactions like titanium silicalites and, in acid-catalyzed reactions like aluminosilicates (7, 8). Unfortunately, the presence of aluminum ions in alumino-titanium silicate (Al-TS-2) molecular sieves has been reported to be detrimental to the oxyfunctionalization of *n*-hexane and to favor the direct H_2O_2 decomposition (7, 8). In addition, the selectivity in acid-catalyzed *m*-xylene isomerization has been found to be affected by the presence of titanium in the framework (8). The choice of boron rather than aluminium might appear more promising for the oxidation properties since this element generates much weaker acidity than aluminum (3, 4). Up to now, all the available evidence of the simultaneous incorporation of titanium and aluminum or iron in a silicalite framework are indirect. Since both the oxidation and the acid functions depend on whether the ions are in framework or extraframework positions, it is very important to identify the phases generated by a simultaneous incorporation of foreign atoms in the framework and relate the activity with the structure.

This work deals with the direct synthesis of titanium boralites with MFI structure (TBS-1). The simultaneous incorporation is characterized using XANES, IR, and UV–visible spectroscopies combined with XRD measurements. The reactivity and boron NMR studies will be reported later (9).

2. EXPERIMENTAL

A series of TBS-1 catalysts was prepared keeping constant the boron concentration and varying the titanium and the hydrogen peroxide concentrations in the initial mixture. The synthesis of titanium boralites was carried out from tetraethyl-orthosilicate (TEOS), tetraethylorthotitanate (TEOT), and boric acid provided by Aldrich. The templating agent, an alkali-free tetrapropylammonium hydroxide (TPAOH), was prepared in our laboratory.

Two solutions were prepared separately. TEOT (0.69 g) was added to doubly distilled water (18.6 g) whereupon a white precipitate (hydrous titanium oxide) was formed. An aqueous H_2O_2 (1.89 g; 30 wt%) was added to the slurry at room temperature. Vigorous stirring conditions were maintained for 2 h to reach the point of complete dissolution of the oxide. This first solution was characterized by

[1] To whom correspondence should be addressed.

0021-9517/95 $12.00

a strong yellow coloration which attested the formation of soluble peroxytitanates. A second solution was made from TEOS (21.5 ml) wherein was added three-fourths of the required amount of template, i.e., 36 ml of a 20 wt% aqueous solution of TPAOH. Then, a solution containing boric acid (1.2 g) in water (40 g) was added dropwise under vigorous stirring. The stirring of the solution was maintained for 15 min in order to complete the hydrolysis of TEOS followed by the addition of the last fourth of the TPAOH solution (12 ml). This mixture was stirred at 333–343 K for about 3 h to remove the alcohol generated by hydrolysis of TEOS. Finally, solution 1 was added dropwise to solution 2 at room temperature. The pH was fixed to about 11 by addition of ammonium hydroxide. The gel composition was

$$0.40\text{TPAOH}\text{–}x\text{TiO}_2\text{–}0.1\ \text{B}_2\text{O}_3\text{–SiO}_2\text{–}35\text{H}_2\text{O}\text{–}y\text{H}_2\text{O}_2$$

(where $x = 0.00$–0.03 and $y = 0.04$–0.4).

The gel was charged into a Teflon-lined autoclave and heated at 448 K for 5 days. The solid obtained was filtered, washed with distilled water, dried, and calcined at 823 K for 4 h in static air. The Ti and B contents of the sample were determined by FAAS (flame atomic absorption spectroscopy) and ICPAES (induced coupled plasma atomic emission spectroscopy), respectively.

The Ti K-edge X-ray absorption spectra were collected at the radiation synchrotron facility of the LURE (France) and treated as previously described (10–12). The white radiation was monochromatized by a Si(111) two-crystal monochromator. The normalized XANES spectra were analyzed using a classical edge normalization procedure and energy calibration to the first peak of the K-edge of a titanium foil (13). Dehydrated samples were obtained by evacuation at 573 K in vacuum and transferred under dry argon into a vacuum-tight cell for measurements.

Diffuse reflectance UV–vis spectroscopy was performed using a Perkin-Elmer Lambda 5 spectrophotometer interfaced with an IBM computer and using MgO as a standard.

The X-ray diffraction patterns of the samples were recorded on a Rigaku D-MAX II VC X-ray diffractometer using nickel-filtered Cu $K\alpha$ ($\lambda = 1.5406$ Å) radiation and a graphite crystal monochromator. The unit cell parameters were calculated from XRD spectra using silicon as an internal standard.

3. RESULTS

Synthesis. The B/Si ratio of 20% was kept constant in the gel mixtures for all sample preparations. On the other hand, the H_2O_2/B ratios varied either because the titanium content was varied at a constant H_2O_2/Ti or because it was deliberately changed at constant Ti loading in order to study the influence of H_2O_2 on the preparation of TBS materials (Table 1).

TABLE 1

Chemical Composition of Reactant Gels and Final Crystalline Solids (Atomic Ratios)

	Gel				Zeolite	
Sample	Ti/Si	B/Si	H_2O_2/Ti	H_2O_2/B	Ti/Si	B/Si
1	0.010	0.20	5.0	0.25	0.015	0.030
2	0.010	0.20	10.0	0.5	0.014	0.027
3	0.010	0.20	20.0	1.0	0.014	0.028
4	0.010	0.20	40.0	2.0	0.014	0.027
5	0.020	0.20	5.0	0.5	0.022	0.027
6	0.030	0.20	5.0	0.75	0.034	0.027
7	0.030	0	5.0	—	0.034	0
8	0	0.20	0	0	0	0.029

The Ti/Si ratios were found to be systematically higher in the solids than in the initial gel and the B/Si ratios were found to be drastically lower. Moreover, silicon (dissolved silica) and boron (unreacted) were detected in the mother liquor after crystallization while titanium was absent, which indicates that only a part of boron and not all silicon precursors were involved in the crystallization process. This phenomenon is probably due to the competition between silicon and boron during the crystallization process, explaining a lower yield of silicon incorporation during the hydrothermal synthesis in boralites than in silicalites. The incorporation level of boron in the solids stayed constant at about 2.7% and did not seem to depend on titanium or H_2O_2 content in the initial gel (Table 1). A lower yield of silicon incorporation was also observed with titanium silicalite preparations (TS-1 and TS-2) by Ratnasamy *et al.* (14, 15).

XRD. The X-ray pattern of the silicalites revealed a Pnma-orthorhombic symmetry from which the indexation was performed. With an accuracy of 5% on the XRD peak height and considering that the silicalite (boron- and titanium-free) has 100% crystallized, the crystallinity of the TS, BS, and TBS materials was found to be 95 ± 5%. Therefore, most of the following spectroscopic data were related to the crystallized silicalite phase. The unit cell volume was estimated using [501], [804], and [0 10 0] reflections. No further refinement was attempted since the absolute accuracy of 10 Å^3 (Fig. 1) was sufficient for this study. The 3% boron leads to a decrease of the unit cell from 5335 to 5280 Å^3, which is consistent with previous reports (Table 2, samples 8 and 9) (16, 17). On the other hand, the [1.5]TS-1 (sample 10) exhibits a unit cell expansion of 40 Å^3, in agreement with literature data (18). In samples 1–6 (Table 2), both boron and titanium have been incorporated in the preparation. The unit cell volumes, V, of the

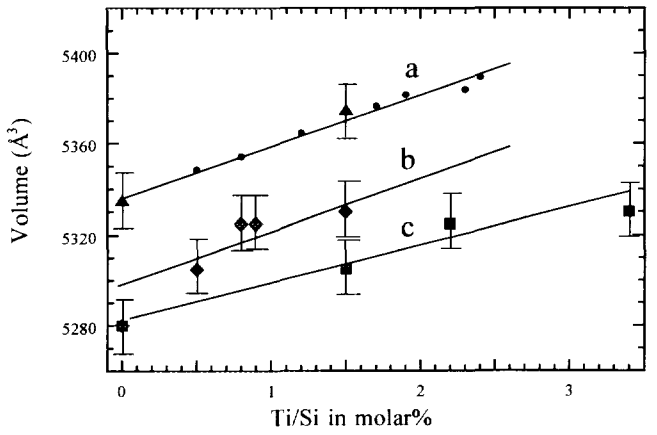

FIG. 1. Evolution of the unit cell volume with the titanium content for: (a) TS1 (▲, this work, ●, Ref. (18)); (b) TBS-1 (◆) versus framework titanium obtained from XANES spectra; and (c) TBS-1 (■) versus total content of titanium.

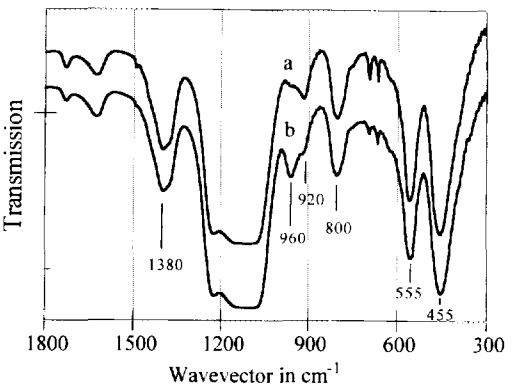

FIG. 2. IR spectrum of: (a) boralite, [2.9]BS; and (b) titanium boralite, [3.4-2.7]TBS.

resulting crystallized materials range between those of the pure S-1 and the 2.9% boron-containing silicalite. Taking the boralite as reference, it is clear that the unit cell progressively expends when the titanium loading, x, increases. A linear fit of the expansion can be proposed as in the case of TS-1 (Figs. 1a and 1c). The slope (dV/dx) associated with the unit cell expansion is smaller for TBS-1 than TS-1 (15 instead of 20 Å^3, respectively) (18). Since only the framework titanium sites contribute to the unit cell expansion, curve 1b is plotted vs the content of those sites, the concentration of which is estimated from the XANES spectra (vide infra). The straight line b (Fig. 1) has been chosen parallel to curve a to ease the discussion of the simultaneous incorporation of B and Ti.

Framework IR. The IR spectra in the 300–1800 cm^{-1} range contain a series of bands which characterize the framework and its modifications by introduction of boron and titanium (Fig. 2). The well-defined IR bands at 800 and 455 cm^{-1} and the saturated region in the 1000–1300 cm^{-1} range are characteristic of SiO_4 tetrahedron units

TABLE 2

Chemical Composition of Crystalline Solids and XANES and XRD Characteristics for Titaniumboralites

Sample	Zeolite	Hydrated[b] Tetra. Ti T/(O + T) (%)	Dehydrated[b] Tetra. Ti T/(O + T) (%)	Dehydrated[b] Tetra. Ti Ti/Si (%)	Dehydrated[b] Octa. Ti Ti/Si (%)	Unit cell[c] volume (Å^3)
1	[1.5-3.0]TBS-0.3[a]	20	35	0.5	1.0	5305
2	[1.4-2.7]TBS-0.5	—	45	0.6	0.8	—
3	[1.4-2.7]TBS-1.0	—	55	0.8	0.6	—
4	[1.4-2.7]TBS-2.0	25	55	0.8	0.6	5325
5	[2.2-2.7]TBS-0.5	25	40	0.9	1.3	5325
6	[3.4-2.7]TBS-0.8	25	45	1.5	1.9	5330
7	[3.4]TS1	30	50	1.7	1.7	5370
8	[2.9]Boralite	—	—	—	—	5280
9	Silicalite-1	—	—	—	—	5335
10	[1.5]TS1	60	100	1.5	0	5375

[a] 1.5 and 3.0% for Ti/Si and B/Si atomic ratios, respectively, in Ti-Boralite with H_2O_2/B = 0.3 in the gel referred to as [1.5-3.0]TBS-0.3.

[b] Percentage of titanium with tetrahedral (T) and octahedral (O) coordination calculated from XANES results with an accuracy of less than ±3%, see text.

[c] Calculated from XRD.

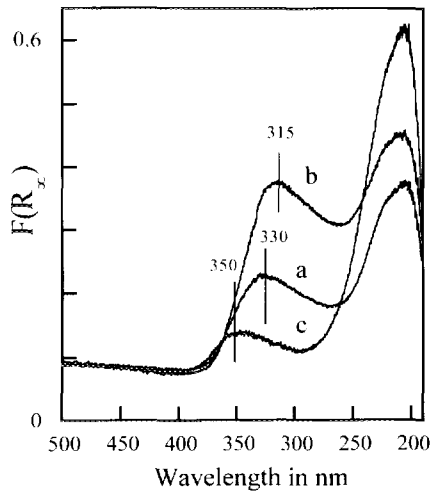

FIG. 3. UV–visible diffuse reflectance spectra of titanium boralites with the same B loading and various titanium loadings (Ti/H_2O_2 being constant in the gel): (a) [1.5-3]TBS; (b) [2.2-2.7]TBS; and (c) [3.4-2.7]TBS.

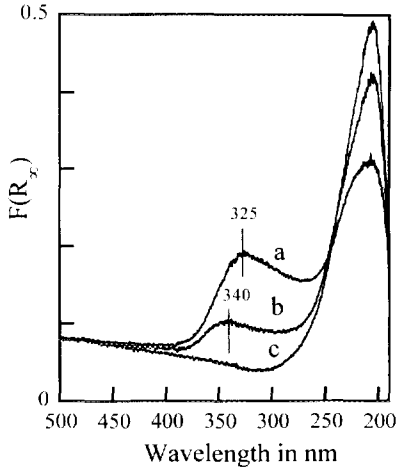

FIG. 4. UV–visible diffuse reflectance spectra of titanium boralites with the same Ti loading and B loadings of 1.5 and 3.0%, respectively, and varying H_2O_2/B ratios: (a) [1.5-3]TBS-0.3; (b) [1.4-2.7]TBS-2.0; and (c) [1.5]TS-1.

while the vibrational mode at 555 cm^{-1} attests the presence of the five member rings of the pentasil silicalites and zeolites (19). The IR bands at 1380 and 920 cm^{-1} are known to characterize tri- and tetracoordinated boron in the framework, respectively (20–22). The IR band at 960 cm^{-1} observed for TBS-1 is used as the fingerprint of the titanium incorporation in boron-free silicalite (23, 24), though it is still a matter of discussion.

UV–vis spectroscopy. The pure boralite [2.9]BS-1 exhibits no UV band in the 200–400 nm range where lie the features of the titanium boralites and TS-1 samples which indeed for the two materials are very similar. Between 270 and 400 nm, the absorption exhibits a broad peak assigned to TiO_2 anatase, while below 270 nm, an intense peak is assigned to isolated titanium species incorporated in the framework (23, 24). The absence of UV bands in the visible region indicates that there is no Ti^{3+} species and that all the titanium lies in the 4+ oxidation state.

The comparison of the UV–visible spectra of [3.4]TS-1 and [3.4-2.7]TBS-1 samples clearly indicates that both samples are quite similar in terms of quantity and type of extraframework species with a peak maximum at 350 nm typical of bulky titanium dioxide, TiO_2. Extraframework species with UV characteristics different from those of bulk TiO_2 (maxima at 330 and 315 nm) are found in the samples 2 and 5, which contain less titanium (Fig. 3). The blue shift of the maximum clearly indicates a change in the nature of extraframework species. Relying on the UV band intensity, it seems that having less titanium in the gel leads to a lower incorporation yield of Ti. This is very surprising since the reverse trend is observed for TS-1. Nevertheless, it is worth noting that less Ti also means less H_2O_2 in the gel (H_2O_2/B = 0.3, 0.5, and 0.8 for 1.5, 2.2, and 3.4 mol% Ti, respectively). This raises the question of the effect of hydrogen peroxide concentration on the type and the quantity of extraframework species formed during the hydrothermal synthesis. The series of titanium boralites prepared with varying H_2O_2/B ratios at a fixed titanium loading of 1.4 mol% Ti (samples 1–4) was therefore investigated. The UV–visible spectra of this series exhibit a band in the 270–400 nm region, the intensity of which decreases when more H_2O_2 is added to the preparation gel up to a H_2O_2/B ratio of 2.0 (Fig. 4). This is apparently consistent with a diminution of extraframework Ti concentration when an excess of hydrogen peroxide is added. Like in the previous series, the UV bands of extraframework titanium is blue shifted in comparison with the position expected for bulk TiO_2. In addition, the titanium loading chosen for these samples is low enough to avoid the formation of extraframework Ti species in boron-free TS-1 samples as indicated by the absence of UV bands in the 270–400 nm range for [1.5]TS-1 (Fig. 4). Conversely, the systematic presence of a UV band in this region for TBS-1 clearly shows that extraframework Ti species are systematically generated in the presence of boron. In both series, the hydrogen peroxide concentration seems to be an important parameter influencing the extraframework species nature and concentration.

In spite of the difficulty in quantifying UV–visible intensities, the changes in peak intensity below 270 nm are interpreted as reflecting the difference in framework Ti content. In this case, the framework species are more likely to be identical in all samples and therefore the band intensity must be directly proportional to the concentration. Thus it is concluded that framework-incorporated Ti increases in concentration as the titanium loading (Fig. 3)

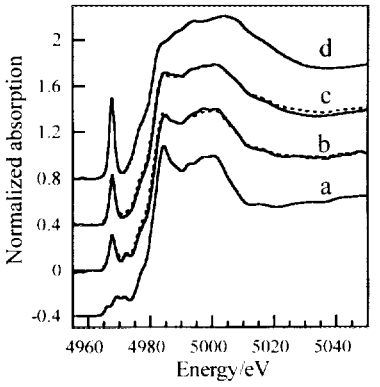

FIG. 5. Ti K-edge XANES spectra of: (a) anatase; (b) [1.5-3.0]TBS-0.3; (c) [1.4-2.7]TBS-2.0; and (d) [1.5]TS-1. Dotted lines indicate the linear combination fits of XANES spectra using as reference spectra those of anatase for octahedral coordination (a) and [1.5]TS-1 for tetrahedral coordination (d).

or hydrogen peroxide concentration (Fig. 4) increases. By contrast, the inconsistent intensity variation of the peak in the 270–400 nm range versus titanium loading indicates that no quantification of this species should be attempted by UV spectroscopies.

XANES. The Ti K-edges of dehydrated and hydrated TBS-1 were compared to those of bulky TiO_2 anatase and dehydrated [1.5]TS-1. The pre-edges of TBS-1 samples exhibit intermediate features compared to the two reference materials (Fig. 5). This suggests the presence of a mixture of sites in the TBS-1 samples. Taking into account the absence of anatase or any form of extraframework Ti in the [1.5]TS-1, the Ti K-edge of this sample was taken as a reference for 100% incorporation of titanium in the framework. Accordingly, the Ti K-edge of anatase was adopted as reference for octahedral titanium. Simulations of the titanium K-edges using a linear combination of the two reference edges led to excellent fits of the dehydrated TBS-1 (Fig. 5, dotted lines). A quantitative determination of tetrahedral and octahedral titanium distribution in TBS-1 samples is proposed on this basis (Table 2).

For dehydrated [1.5-3.0]TBS-0.3 and [1.4-2.7]TBS-2.0, prepared with H_2O_2/B ratios of 0.3 and 2.0, respectively, the edges are significantly different and correspond to a tetrahedral:anatase distribution of 35:65 and 55:45, respectively (Figs. 5b and 5c, sample 1 and 4 in Table 2). The accuracy of these distributions is about ±3%; a difference of 5% is indeed significant in the range of distribution found here where both phase concentrations are high. The increase of incorporation yield in tetrahedral sites (35, 40, and 45%) with increasing titanium loading in the series of sample 1, 5, and 6 (1.5, 2.2, and 3.4%) is also significant (Table 2). These data indeed confirm the trend observed from the UV spectra relying on the band associated to framework species. In the second series, where the hydrogen peroxide concentration was varied at a constant Ti loading, up to 55% of tetrahedral titanium was found for samples made from gels containing a H_2O_2/B higher than 1 (samples 3 and 4, Table 2). For H_2O_2/B ratios of 0.25 or 0.5 (samples 1 and 2, Table 2) the fraction incorporated in T sites is smaller (35 and 45%, respectively). These results confirm that a better incorporation of titanium is obtained for higher hydrogen peroxide concentration up to a ratio of H_2O_2/B = 1, whereas above this value no significant effect was observed. Incidentally, in the first series of samples, the [3.4-2.7]TBS-1 has been prepared from a gel containing a H_2O_2/B ratio of 0.75; its characteristics are effectively close to those of the boron-free [3.4]TS-1 silicalite. According to the XANES fits, the maximum titanium incorporated in the presence of boron is about 1.5%. For hydrated samples, the fit quality was not as good as for dehydrated samples and the confidence on site occupancy was not as reliable. The number of tetrahedral sites was nevertheless estimated and found to be about half of the number obtained for the dehydrated samples.

4. DISCUSSION

Incorporation of Ti and B. It is widely accepted that heteroatoms like Al(III) or B(III) or transition metal ions like Fe(III) can substitute silicon in many minerals. In contrast to most of the silicates, an isomorphous substitution in a zeolite can only take place in tetrahedral sites. Therefore, in addition to the ionic radius limitations, there is a symmetry constrain for the site occupancy. A departure from tetrahedral symmetry is most often interpreted as an indication that the heteroatoms are located in extraframework positions. Nonetheless, if a framework species has to be catalytically active, its coordination number should change in the presence of solvent, reactants, and products. This implies a certain fragility of the site that can be eventually removed from its framework position by drastic treatments. The boron chemistry is dominated by the three and four coordination states. In boralites, tri- and tetracoordinated boron ions are indeed characterized by IR bands at 1380 and 920 cm^{-1}, respectively. The stabilization of boron in the framework during calcination is obtained by replacement of exchangeable H^+ by Na^+ or NH_4^+ ions that maintain the site in a fourfold coordination state (20–22). This is observed in our own boralite and in the titanium boralite as well (9). On the other hand, titanium ions tend to increase their coordination number from 4 to 6. This has been clearly demonstrated by EXAFS spectroscopy for TS-1 where H_2O or NH_3 reversibly adsorb on titanium sites (25–27). A similar trend has been observed in TS-48 (28). Consequently, not only the symmetry but also the reversible evolution of the site and the phase identification are necessary to draw conclusions on the effectiveness of

the heteroatom isomorphous substitution. In titanium boralites, the evolution of the titanium Ti K-edges upon dehydration, like in other types of framework, is a clear indication of the presence of titanium framework species (Fig. 5, Table 2).

The unit cell variations should account for the differences in ionic radii of Ti^{4+}, Si^{4+}, and B^{3+} and, consequently, for M–O distances (1.79, 1.61, and 1.47 Å for $M = Ti^{4+}, Si^{4+}$, and B^{3+}) (18, 29, 30). Accordingly, the [2.9]BS-1 sample exhibits a contraction consistent with the literature (16, 17). The unit cell expansion undergone by the silicalite framework in the [1.5]TS-1 is consistent with a sample free of extraframework species (Fig. 1) and with the absence of UV bands in the range of 270–400 nm. A mixed effect is observed for the two series of titanium boralites for which unit cells larger than pure boralite [2.9]BS-1 and smaller than pure silicalite S-1 unit cell were found (Table 2). This clearly shows that boron is more or less incorporated but, for titanium, the proof is not established on these data only. Indeed, a unit cell volume smaller than that of S-1 might be obtained in the complete absence of framework titanium or with a range of Ti/B ratios. However, the presence of an intense band in the range 200–270 nm is consistent with titanium framework species in TBS-1, like in the [1.5]TS-1 sample, and with other reports (23, 24).

Though the IR and UV spectra of TBS-1 present features of both TS-1 and boralite, this is not a proof of simultaneous incorporation. On the other hand, the presence of segregated grains of TS-1 and BS-1 phases would yield dual XRD patterns. The observed patterns for our TBS-1 samples, which show well-crystallized single phase and no line broadening, strongly suggest that Ti and B are simultaneously incorporated in the silicalite framework.

Nature of the sites. The absence of any new IR features in the titanium boralites other than the IR bands at 1380, 960, and 920 cm^{-1} assigned to boralite or TS-1 phases may indicate that, despite the presence of the two elements in the same crystallites, there are no mixed Ti–B sites in the framework. This raises the question of the assignment of these bands and their relation to the type of sites in TBS-1.

The more accepted assignment for the 960 cm^{-1} was originally formulated by Boccuti *et al.* [23], who claimed that it is due to a local vibrational mode of the asymmetric stretching of the SiO_4 tetrahedral unit linked to a titanium ion. This normal mode is threefold degenerated in the T_d symmetry and split into two normal modes in the C_{3v} symmetry, the local mode being predominantly described as a (O_3Si)–(OTi) vibration. According to FT-IR spectrum differences obtained from S-1 and TS-1, there are in fact three new vibrational modes at 965, ~1080, and ~1200 cm^{-1} (10). The lowering of symmetry can be considered to continue even further, down to C_{2v} or C_s. The first two peaks are indeed Raman active according to the measurements made by Deo *et al.* (31). Along this reasoning, one may deal with not only one but two Si–O–Ti bridges per Si, i.e., a double oxo bridge between Ti and Si. This interpretation is consistent with a very short Ti–Si bond distance of 2.2–2.3 Å calculated from EXAFS in TS-2 or TS-1, implying that the Ti site would be a framework defect rather than a substitutional one (11, 12, 26). However, this hypothesis has received little support from other EXAFS studies (27, 32). Recently, Camblor *et al.* have proposed an alternative explanation for the local vibrational mode which would be due to a $Si–O^-$ group with counterions that could be either H^+, the protonated template, and/or Na^+ (33). Khouw and Davis state that by reaction with an aqueous NaOH solution, TS-1 gives rise to TiOH and SiONa groups, causing the disappearance of the 960 cm^{-1} band and the appearance of a 985 cm^{-1} band assigned to SiONa groups (34). The latter group would be formed by sodium exchange of a SiOH group adjacent to TiOH groups. It is not yet established if these groups naturally occur in TS-1, implying that some of the Ti–O–Si bridges are left open in the starting material, or if they are generated by hydrolysis of these bridges during the reaction with NaOH. It is therefore not excluded that the 960 cm^{-1} band might be due to those SiOH adjacent to titanium sites in TS-1. Along the same line of reasoning, the band at 920 cm^{-1} would be due to a Si–OH group adjacent to a boron site. The vibrational Si–OH local mode of the silanol undergoes a red shift more likely due to a donation of an oxygen doublet that forms the fourth coordination of boron (20). Additional evidence that the band at 960 cm^{-1} is not characteristic of the Ti element only, is that the same band has been reported to be present in Cr-silicalite (35) and in V-silicalite (36). Whatever the discrepancy in the interpretations, it seems that the characteristic IR bands are due to a modification of SiO_4 units indirectly related to the presence of titanium or boron in absence of other heteroatoms such as Cr or V. Furthermore, there is no indication that they necessarily imply framework species; very similar bands are observed in borosiloxane or titaniumsiloxane polymers (37) in mixed oxides (38) or in TiO_2 grafted on silica (39). Therefore, the IR bands are rather a fingerprint of heteroatoms on a matrix of $[SiO_4]$ units whatever its crystallization state. By contrast, XPS or XANES at the Ti K-edge bring direct information on the titanium symmetry and environment. Similarities between titanium sites in titanium glasses and TS-2 have been proposed according to these latter techniques (12).

The Ti-edge profiles are recognized as a very sensitive tool to a local symmetry (pre-edge) and long range environment (postedge) (40). A given phase has a characteristic edge that allows one to differentiate tetracoordinated from pentacoordinated or hexacoordinated titanium in Ba_2TiO_4, fresnoite, or anatase (32, 41, 42). One also easily makes out the difference between octahedral titanium sites

in the various TiO_2 phases, rutile, brookite, and anatase. Identification of anatase and tetrahedral Ti^{4+} in titanium glasses or in silica-supported TiO_2 has been obtained from Ti K-edge analysis (43, 44). Tetrahedral TiO_4 sites also exhibit different Ti K-edges in different phases such as Ba_2TiO_4 and hexadecaphenyl-octosiloxyspiro(9,9) titanium(IV), HDPOSST (10). The latter compound has a core made of a tetrahedral $Ti–O(Si)_4$ unit that mimics a true substitutional site in silica or silicalite. Based on the similarity of the Ti K-edge of HDPOSST and TS-1, a true substitutional site is more likely to occur in TS-1 (45). This conclusion is supported by the Ti–O–Si angle estimated to be 160° using multiple scattering calculations of the EXAFS oscillations (45). The apparent discrepancy with our previous conclusions based on EXAFS data (10–12, 26) might be attributed to the improvement of data quality, comparison with an appropriate model compound, a new calculation technique, and careful control of the dehydration level during data acquisition. However some of our previous IR results regarding the splitting of the asymmetric stretching of the SiO_4 unit are still not explained by the conventional substitution model.

In titanium boralites, the edges vary depending on the extraframework species concentration. The presence of anatase is ascertained by the characteristic triplet at about 20 eV above the edge. Assuming tetrahedral framework species like in TS-1, the simulations of the dehydrated TBS-1 were performed using a linear combination of the edge of [1.5]TS-1 free of the extraframework species and the edge of anatase. The strikingly good match between the simulated and the experimental spectra clearly suggests that TBS-1 contains the same titanium sites as TS-1 (Fig. 5). Furthermore, it confirms that the extraframework species are located in a separate anatase phase. This latter conclusion is in agreement with Raman studies (39).

As mentioned above, the Ti K-edge of titanium boralites is modified upon hydration. This is attributed to a change of symmetry more likely due the addition of a water molecule in the coordination sphere of titanium (25, 26). A recent EXAFS study of TS-1 reveals that the change in Ti coordination occurs reversibly at room temperature for NH_3 instead of 200°C for H_2O (27). The edge and the symmetry of the hydrated sites are not known. As a consequence, the simulation performed on the hydrated titanium boralite edges is not rigorous because the hydrated sites were tentatively fitted with inadequate references leading indeed to lower fit quality. It may be presumed that tetrahedral, square pyramidal, and octahedral symmetry of Ti coexist in hydrated samples, in agreement with previous findings for TS-1 and TS-2 samples (11, 12, 25, 42, 46). The UV absorption at 210 nm was assigned to tetrahedral sites while the absorption at 230 nm was ascribed to isolated octahedral titanium species (6, 24). However, it might well be that this shoulder corresponds to pentacoordinated titanium produced by partial hydration of framework species.

The last striking point to discuss is the blue shift of the UV band associated to extraframework species which has been also observed in titanium beta-boralites (6). The Ti^{4+} ions have a d^0 electronic configuration; no d–d nor metal-to-ligand transitions are expected. Consequently, all the UV bands are assigned to ligand-to-metal charge transfer (LMCT) (47). It has been observed for V^{5+} and Mo^{6+} ions that the larger the size of the polyoxoanions the lower the LMCT frequency (48). Conversely, the smaller the oxide cluster trapped in an amorphous glass, the higher the frequency of the LMCT. This so-called quantum size effect associated to a blue shift has been observed in many different cases comprising Ti–Si mixed oxides or silica supported TiO_2 (38, 49). The blue shift of the UV band from 350 (bulky anatase) to 330 nm for sample (b) and to 315 nm for sample (a) in Fig. 4 (from 340 to 325 nm in Fig. 3) is more likely due to a decrease in the size of oxide clusters along this series of samples. The edge analysis reveals that they have an anatase structure. This blue shift is not observed in TS-1 samples. It seems that in the presence of boron the nucleation growth of the oxide cluster is limited while the number of nuclei increases (referring to the higher content of extraframework Ti). The small oxide clusters are more likely formed during calcination and trapped within the framework cavities; further studies are necessary to clarify this point.

Quantification of framework Ti species. The K-edges are characterized by a step the height of which is proportional to the number of titanium atoms in the sample, allowing their normalization to the step height. Since each phase has its own edge signature, a quantitative treatment of the edge is possible in the case of phase mixtures. Indeed, the simulation of the TBS-1 edges using a linear combination of the [1.5]TS-1 and anatase TiO_2 reflects the phase composition of each dehydrated sample. Keeping in mind that the first reference contains only framework species and the second corresponds to a well-defined TiO_2 phase associated to extraframework species, the T and O site distribution in dehydrated samples corresponds also to framework versus extraframework distribution. The titanium edges of TS-1 were simulated using HDPOSST and anatase as reference compounds (45). Tetrahedral Ti sites were estimated to represent 70% and 35% of titanium in the silicalite for loadings of 2.4 and 4.6 mol% Ti, respectively. The rest of the titanium is characterized as an anatase phase, consistent with previous Raman studies (31). These figures are consistent with an incorporation limit of about 1.8 mol% Ti in the TS-1 framework determined independently from XRD (50) and voltametric measurements (51) or by indirect titration of extraframework TiO_2 using Raman spectroscopy (31). Using the [1.5]TS-1 for

tetrahedral reference instead of HDPOSST leads, within 5%, to the same results for TS-1 or TBS-1.

The unit cell of the TBS-1 samples is been reported in Fig. 1 as a function of their calculated framework Ti loading (Table 2). Taking into account that the titanium sites are identical in TBS-1 and in TS-1, one expects that the unit cell expansion slope, dV/dx is the same for boralites and silicalites at constant boron framework concentration. A straight line parallel to the line obtained for TS-1 unit cell expansion has been drawn in Fig. 1 (line b) as a guideline for discussion. For a given Ti framework content, it appears that all TBS-1 samples have a smaller volume than the TS-1 sample (line a). The difference in volume is nevertheless smaller by about 2/3 of the difference between the pure silicalite and the boralite (line a and line b at Ti/Si = 0). This might be due to a lower defect concentration in the TBS-1 than in the boralite. Since the presence of more heteroatoms in the framework is not likely to decrease the defect concentration in the structure, the reason is to be found in a lower boron concentration by about the 2/3 of its level in the [2.9]BS-1 used as the reference (Ti/Si = 0, Fig. 1).

Effect of hydrogen peroxide on the preparation. From XANES and UV–visible data, it is clear that for samples made from gels with low H_2O_2/B ratios, there is more extraframework titanium species. This can be explained by the irreversible formation of TiO_2 in the gel before crystallization, due to the destruction of peroxytitanate in the presence of boric acid. Indeed, boric acid reacts with the excess of H_2O_2 necessary to stabilize peroxytitanate and decreases the solubility of titanium. It must therefore be noticed that the solubilization of titanium in the gel is key for avoiding the formation of TiO_2. When the H_2O_2/B mole ratio was decreased from 2.0 to 0.3, most probably, a small amount of titanium oxide was produced from soluble peroxytitanates caused by the formation of peroxoborates in the reaction mixture according to reaction [1] and [2] (52).

Once formed, the TiO_2 does not dissolve back under the hydrothermal conditions. It is therefore important to prevent the formation of precipitates in the gel.

$$Ti(OC_2H_5)_4 \xrightarrow{H_2O} \underset{\text{(white precipitate)}}{Ti(OH)_4} \xrightleftharpoons{H_2O_{2(aq)}} [TiO_2(OH)(H_2O)_2]OH \quad [1]$$

$$H_3BO_3 \xrightarrow{OH_{(aq)}} B(OH)_4^- \xrightleftharpoons{H_2O_{2(aq)}} [B(OH)_3OOH]^- + H_2O \quad [2]$$

5. CONCLUSION

The effects of hydrogen peroxide on the simultaneous incorporation of Ti and B in silicalites of MFI structure have been monitored using XRD measurements, XANES, XRD, IR, and UV–vis spectroscopies. The lattice contraction clearly demonstrates that the incorporation of boron occurs. Conversely, at a constant content of boron, a linear correlation between the titanium content and the unit cell expansion evidences that incorporation of titanium takes place in the presence of boron. This interpretation is sustained by the IR spectra revealing a characteristic band at 960 cm^{-1} of an heteroatom i.e., titanium in the silicalite framework and those of boralites at 920 and 1380 cm^{-1}. The UV–visible spectra of these titanium boralites reveal the presence of Ti extraframework species with a broad UV band in the 270–400 nm range that is characterized by a maximum and an intensity depending on the H_2O_2/B ratio. From the titanium K-edges, these are identified as TiO_2 anatase clusters of varying size, the smaller being associated to the more blue-shifted UV bands.

According to the TBS-1 edges, the framework tetrahedral sites are similar to those in titanium silicalites. A semiquantitative analysis by edge fitting using a linear combination of both anatase and [1.5]TS-1 edges allows one to obtain a site distribution. The highest incorporation level of Ti into the framework was estimated to be 1.5 mol%. The best incorporation yields were obtained for hydrogen peroxide-to-boron molar ratios in the gel close to one or higher. Below this value, it is believed that the excess of hydrogen peroxide is not sufficient to stabilize the soluble peroxytitanate that precipitates as TiO_2 or titanium hydroxide clusters in the gel. This is attributed to the consumption of a part of the hydrogen peroxide by formation of boron peroxide. The hydrogen peroxide concentration had no effect on the substitution level of boron. The presence of boron in the framework does not significantly affect the limit of incorporation of titanium. It is also not yet clear if it is possible to prepare titanium boralites free of extraframework Ti.

ACKNOWLEDGMENTS

We thank Dr. C. Cartier for numerous discussions and for help with the XAFS data acquisition. Support of this work was provided by a Strategic Grant from the NSERC.

REFERENCES

1. Bellussi, G., European Patent A1 0 272 496, 1987.
2. Bellussi, G., Carati, A., Clerici, M. G., and Esposito, A., *Stud. Surf. Sci. Catal.* **63,** 421 (1991).

3. Lam Shang Leen, K. K., U.S. Patent 4, 623, 526 and U.S. Patent 4, 519, 998, 1985.
4. Lam Shang Leen, K. K., and Jin Rong, Ch., European Patent B1 0 148 038, 1984
5. Forni, L., and Pelozzi, M., *J. Mater. Chem.*, 1101 (1990); Forni, L., Pelozzi, M., Guisti, A., Fornasari, G., and Millini, R., *J. Catal.* **122,** 44 (1990).
6. Rigutto, M. S., de Ruiter, R., Niederer, J. P. M., and Van Bekkum, H., *Stud. Surf. Sci. Catal.* **84,** 2245 (1994).
7. Thangaraj, A., Kumar, R., and Ratnasamy, P., *Appl. Catal.* **57,** L1, (1991); Thangaraj, A., Sivasanker, S., and Ratnasamy, P., *Zeolites* **12,** 135 (1992).
8. Reddy, J. S., Kumar, R., and Csicsery, S. M., *J. Catal.* **145,** 73 (1994).
9. Trong On, D., Kapoor, M. P., Bonneviot, L., Kaliaguine, S., Gabelica, Z., *J. Chem. Soc., Faraday Trans.*, submitted for publication.
10. Trong On, D., Denis, I., Lortie, C., Cartier, C., and Bonneviot, L., *Stud. Surf. Sci. Catal.* **83,** 101 (1994).
11. Trong On, D., Bittar, A., Sayari, A., Kaliaguine, S., and Bonneviot, L., *Catal. Lett.* **16,** 85 (1992).
12. Trong On, D., Bonneviot, L., Bittar, A., Sayari, A., and Kaliaguine, S., *J. Mol. Catal.* **74,** 223 (1992).
13. Michalowicz, A., *in* "Structures Fines d'Adsorption X en Chimie," Vol. 3 (H. Dexpert, A. Michalowicz, and M. Verdaguer, Eds.). CNRS, Orsay, 1990.
14. Thangaraj, A., Sivasanker, S., and Ratnasamy, P., *J. Catal.* **131,** 294 (1991).
15. Reddy, J. S., Sivasanker, S., and Ratnasamy, P., *J. Mol. Catal.* **71,** 373 (1992).
16. Meyers, B. L., Ely, S. R., Kutz, N. A. Kaduk, J. A., and Van Den Bossche, E., *J. Catal.* **91,** 352 (1985).
17. Mirajkar, S. P., Thangaraj, A., and Shiralkar, V. P., *J. Phys. Chem.* **96,** 3073 (1992).
18. Perego, G., Bellussi, G., Corno, C., Taramasso, M., Buonomo, F., Esposito, A., *Stud. Surf. Sci. Catal.* **28,** 129 (1986).
19. Miecznikowski, A., and Hanuza, J., *Zeolites* **7,** 249 (1987).
20. Coudurier, G., Auroux, A., Védrine, J. C., Farlee, R. D., Abrams, L., and Shannon, R. D., *J. Catal.* **108,** 1 (1987).
21. Kessler, H., Chezeau, J. M., Guth, J. L., Strub, H., and Coudurier, G., *Zeolites* **7,** 360 (1987).
22. Scarano, D., Zecchina, A., Bordiga, S., Geobaldo, F., Spoto, G., Petrini, G., Leofanti, G., Padovan, M., and Tozzola, G., *J. Chem. Soc. Faraday Trans.* **89,** 4123 (1993).
23. Boccuti, M. R., Rao, K. M., Zecchina, A., Leofanti, G., and Petrini, G., *Stud. Surf. Sci. Catal.* **48,** 133 (1989).
24. Zecchina, A., Spoto, G., Bordiga, S., Ferrero, A., Petrini, G., Leofanti, G., and Padovan, M., *Zeolite Chem. Catal.*, 251 (1991).
25. Lopez, A., Kessler, H., Guth, J. L., Tuiler, M. H., and Topa, J. M., "Proceedings, 6th International Conference on X-ray Absorption Fine Structure, York," p. 549, 1990.
26. Bonneviot, L., Trong On, D., and Lopez, A., *J. Chem. Soc. Chem. Commun.*, 685 (1993).
27. Bordiga, S., Coluccia, S., Lamberti, C., Marchese, L., Zecchina, A., Boscherini, F., Genoni, F., Leofanti, G., Petrini, G., and Vlaic, G., *J. Phys. Chem.*, **98,** 4125 (1994).
28. Reddy, K. M., Kaliaguine, S., Sayari, A., Ramaswamy, A. V., Reddy, V. S., and Bonneviot, L., *Catal. Lett.* **23,** 175 (1994).
29. Krogh-Moe, J., *Acta Cristallogr. B* **28,** 169 (1972).
30. Mesline, S., and Santoni, F., *Acta Cristallogr. B* **28,** 3559 (1972).
31. Deo, G., Turek, A. M., Wachs, I. E., Huybrechts, D. R. C., and Jacobs, P. A., *Zeolites* **13,** 365 (1993).
32. Pei, S., Zajac, G. W., Kaduk, J. A., Faber, J., Boyanov, B. I., Duck, D., Fazzini, D., Morrison, T. I., and Yang, D. S. *Catal. Lett.* **21,** 333 (1993).
33. Camblor, M. A., Corma, A., and Perez-Pariente, J., *J. Chem. Soc. Chem. Commun.*, 685 (1993).
34. Khouw, C. B., and Davis, M. E., *J. Catal.* **151,** 77 (1995).
35. Chapus, T., Tuel, A., Ben Taârit, Y., and Naccache, C., *Zeolite* **14,** 349 (1994).
36. Hari Prasad Rao, M. R., and Ramaswamy, A. V., *J. Chem. Soc. Chem. Commun.*, 1245 (1992).
37. Abe, Y., Gunji, T., Kimata, Y., Kuramata, M., Kasgöz, A., and Misono, T., *J. Non-Cryst. Solids* **121,** 21 (1990).
38. Liu, Z., and Davis, R. J., *J. Phys. Chem.* **98,** 1253 (1994).
39. Srinivasan, S., Datye, A. K., Hampden-Smith, M., Wachs, I. E., Deo, G., Jehng, J. M., Turek, A. M., and Peden, C. H. F., *J. Catal.* **131,** 260 (1991).
40. Cartier, Ch., Momenteau, M., Dartyge, E., Fontaine, A., Tourillon, G., Michalowicz, A., and Verdaguer, M., *J. Chem. Soc. Dalton Trans.*, 609 (1992).
41. Yarker, C. A., Johnson, P. A., Wright, A. C., Greegor, B., Lytle, F. W., and Sinclair, R. N., *J. Non-Cryst. Solids* **70,** 117 (1986).
42. Behrens, P., Felsche, J., Vetter, S., Schultz-Ekloff, G., Jaeger, N. I., and Niemann, W., *J. Chem. Soc. Chem. Commun.*, 678 (1991).
43. Greegor, B., Lytle, F. W., Sandstrom, D. R., Wong, J., Schultz, P., *J. Non-Cryst. Solids* **55,** 27 (1983).
44. Salama, T. M., Tanaka, T., Yamaguchi, T., and Tanabe, K., *Surf. Sci. Lett.* **227,** L100 (1990).
45. Cartier, C., Lortie, C., Trong On, D., Dexpert, H., and Bonneviot, L., *Physica B,* **208–209,** 653 (1995).
46. Geobaldo, F., Bordiga, S., Zecchina, A., Giamello, E., Leofanti, G., and Petrini, G., *Catal. Lett.* **16,** 109 (1992).
47. Lever, A. B. P., "Inorganic Electronic Spectroscopy," 2th ed., p. 203. Elsevier, Amsterdam, 1984.
48. Weber, R. S., *J. Catal.* **152,** 470 (1995).
49. Lassoletta, G., Fernandez, A., Espinos, J. P., and Gonzalez-Elipe, A. R., *J. Phys. Chem.* **99,** 1484 (1995).
50. Millini, R., Previde Massara, E., Perego, G., and Bellussi, G., *J. Catal.* **137,** 497 (1992).
51. Castro-Martins, S., Tuel, A., and Ben Taârit, Y., *Stud. Surf. Sci. Catal.* **84,** 501 (1994).
52. Cotton, F. A., and Wilkinson, G., "Advanced Inorganic Chemistry," 4th ed., p. 699. Wiley, New York, 1980.